The Astrophysical Journal, 615:662–674, 2004 November 10

TIME-DEPENDENT CIRCULATION FLOWS: IRON ENRICHMENT IN COOLING FLOWS WITH HEATED RETURN FLOWS

William G. Mathews,[1] Fabrizio Brighenti,[1,2] and David A. Buote[3]
Received 2004 May 18; accepted 2004 July 16

ABSTRACT

We describe a new type of dynamical model for hot gas in galaxy groups and clusters in which gas moves simultaneously in both radial directions. The observational motivations for this type of flow are compelling. X-ray spectra indicate that little or no gas is cooling to low temperatures. Bubbles of hot gas typically appear in *Chandra* X-ray images and *XMM-Newton* X-ray spectra within ~50 kpc of the central elliptical galaxy. These bubbles must be buoyant. Furthermore, the elemental composition and total mass of gas-phase iron observed within ~100 kpc of the center can be understood as the accumulated outflow of most or all of the iron produced by Type Ia supernovae in the central galaxy over time. This gaseous iron has been circulating for many gigayears, unable to cool. As dense inflowing gas cools, it produces a positive central temperature gradient, a characteristic feature of normal cooling flows. This gas dominates the local X-ray spectrum but shares the total available volume with centrally heated, outflowing gas. Circulating flows eventually cool catastrophically if the outflowing gas transports mass but no heat; to maintain the circulation both mass and energy must be supplied to the inflowing gas over a large volume, extending to the cooling radius. The rapid radial recirculation of gas within ~50 kpc results in a flat core in the gas iron abundance, similar to many group and cluster observations. We believe the circulation flows described here are the first gasdynamic, long-term evolutionary models that are in good agreement with all essential features observed in the hot gas: little or no gas cools as required by *XMM* spectra, the gas temperature increases outward near the center, and the gaseous iron abundance is about solar near the center and decreases outward.

Subject headings: cooling flows — galaxies: active — galaxies: clusters: general — galaxies: elliptical and lenticular, cD — X-rays: galaxies — X-rays: galaxies: clusters

1. INTRODUCTION

Now that we have become accustomed to referring to the hot gas in groups and clusters of galaxies as "cooling flows," no cooling gas has been observed. Although energy is lost by X-ray emission, the absence of spectral evidence for gas cooling to low temperatures has been well documented in many observational papers (e.g., Peterson et al. 2001; Xu et al. 2002). The hot gas in groups and clusters of galaxies may cool, but at a much lower rate than previously thought. This has led to numerous theoretical models in which the gas is assumed to be reheated in some fashion: by powerful radio jets, by rising bubbles, by shocks, by magic, etc. Most or all of these models have been unsatisfactory at some level. The most common difficulty of heated flows is not reproducing the observed radial temperature and density profiles (e.g., Brighenti & Mathews 2002, 2003), which are smooth and approximately similar for galaxy clusters of all scales. Less theoretical effort has been expended in understanding the radial abundance gradients in the hot gas, and it is fair to say that little progress has been made so far on this important problem.

In this paper we show that a combination of heating and radial mass redistribution can satisfy these stringent observational constraints and simultaneously explain the observed radial metallicity profiles. While the flows described here retain some useful features of traditional cooling flows, we refer to them as "circulation flows" since gas flows in both directions simultaneously. Cooling to low temperatures is greatly or entirely eliminated. The primary source of heat that drives the circulation is assumed to be moderate active galactic nucleus (AGN) activity in the cores of luminous elliptical galaxies that reside at or near the center of the diffuse X-ray emission in groups and poor clusters.

Our theoretical and observational studies of the virialized hot gas in galaxy clusters have been motivated in several ways. First, we have maintained that hot gas in galaxy groups is more likely to reveal the physical nature and dynamical evolution of the gas than hotter gas in rich clusters. We assume that some of the groups are old and, if cosmically isolated, are less likely to have been upset and mixed by recent mergers or powerful radio sources. Second, we have argued that the radial variation of the gaseous iron abundance in these groups retains an imprint of the origin and dynamical evolution of the gas since it received its iron. Finally, at the relatively low temperatures of gas in galaxy groups, $kT \sim 1$ keV, the influence of thermal conductivity $\kappa \propto T^{5/2}$ on the scale of the flow can be ignored.

In many galaxy groups and clusters the gas-phase iron abundance has a noticeable peak centered on the central elliptical galaxy that extends out to ~100 kpc. The iron abundance increases to approximately solar at the center. *XMM* spectra indicate that 70%–80% of this iron was formed in Type Ia supernovae (SNeIa). Of particular interest for our discussion here is the realization that the total amount of gas-phase iron in this central region is comparable to the total amount of iron

[1] University of California Observatories/Lick Observatory, Department of Astronomy and Astrophysics, University of California, Santa Cruz, CA 95064; mathews@ucolick.org.
[2] Dipartimento di Astronomia, Università di Bologna, via Ranzani 1, Bologna 40127, Italy; brighenti@bo.astro.it.
[3] Department of Physics and Astronomy, University of California at Irvine, 4129 Frederick Reimes Hall, Irvine, CA 92697; buote@uci.edu.

that could be created by all SNeIa in the central galaxy since its stars were formed. This is only possible if little or none of the iron-enriched gas has cooled. It is also significant that the region of enhanced iron emission around the central galaxy is much larger in extent than the half-light radius of the optical galaxy.

To explain these important features, we describe a simple time-dependent model for the long-term evolution of hot gas in galaxy groups in which gas enriched by SNeIa inside the central galaxy is heated and buoyantly transported far into the surrounding gas, where it is stored over time. Meanwhile, most of the hot X-ray–emitting gas loses energy and flows inward, as in a standard cooling flow. The cooling inflow receives both iron-enriched gas and energy from clouds or bubbles of heated gas that are moving outward. To avoid flows with catastrophic cooling or discordant temperature profiles, it is essential that the inflowing gas receive both energy and mass from the central regions. The physical nature of this heating, $P\,dV$ compression, sound wave dissipation, weak shocks, etc., is left unspecified for the time being. For successful flows the mass and energy deposition must be spatially broad, not concentrated near a single radius in the flow. This can be accomplished if inflowing gas arriving near the central galaxy is heated to a variety of entropy levels and ultimately floats upward to approximately that radius at which its entropy matches that of the surrounding, inflowing gas.

The discussion below is a time-dependent generalization of the steady state circulation flows that we discussed in a previous paper (Mathews et al. 2003). Flows in which gas moves in both radial directions at each radius are notoriously difficult to reproduce faithfully even with the most sophisticated multidimensional numerical codes because numerical diffusion across the Eulerian grid blurs the distinction between the counterstreaming flows. For this reason, in this initial study of the time-dependent evolution of radially circulating gas, we study the evolution of the inward flowing gas with a standard Eulerian code but simplify our treatment of the outflowing gas, which is difficult to resolve on computational grids. The physical processes by which gas near the central elliptical galaxy is heated are left unspecified. Some of the less important aspects of bubble dynamics that we discussed in our study of steady state circulation flows—such as momentum exchange by the drag interaction of rising bubbles or the expansion of individual bubbles—are not treated in detail here or are represented by source terms in the equations for the inflowing gas. Since the dynamical time for buoyant gas is much less than the radiative cooling time, we assume that heated outflowing clouds move rapidly to their final destination. Nevertheless, we do not expect that the detailed inclusion of these complications will alter the basic character—or the success—of the circulation flows described here.

We show that time-dependent circulation flows can quite naturally produce all of the major observed radial profiles in the hot gas: its temperature, density, and metallicity. In addition to these important attributes, our circulation flows are compatible with the X-ray observation that very little if any gas cools to low temperatures.

2. OBSERVATIONS OF IRON-ENRICHED HOT GAS IN GALAXY GROUPS

A common feature of well-studied X-ray–luminous galaxy groups is an extended region of enhanced iron emission surrounding the central elliptical galaxy (e.g., Buote et al. 2003a, 2003b; Sun et al. 2003; Xue et al. 2004; Kim & Fabbiano 2004). Typically, the iron abundance is near solar within 30–40 kpc of the center and decreases outward within 100–150 kpc. The ratio of α/Fe elements suggests that a large fraction of this iron has been produced by SNeIa. Today the stars in this region from which the SNeIa presumably occurred are located almost entirely within the central elliptical galaxy, with a half-light radius $R_e \sim 10$ kpc that is much smaller than the scale of the iron enrichment in the surrounding gas.

For example, the X-ray–luminous group NGC 5044 consists of a large elliptical galaxy surrounded by a cloud of much smaller galaxies extending to at least 400–500 kpc. At a distance of 33 Mpc, the central galaxy has luminosity $L_B = 4.5 \times 10^{10}\ L_{B,\odot}$, effective radius $R_e = 10.0$ kpc, and total stellar mass $M_{*t} = \Upsilon_B L_B = 3.4 \times 10^{11}\ M_\odot$, where $\Upsilon_B = 7.5$ is the stellar mass-to-light ratio.

The galaxy is surrounded by a huge cloud of hot gas extending to at least 300 kpc. If the hot gas is assumed to have a single phase, its temperature rises from $kT = 0.7$ keV at the center to a maximum of $kT \approx 1.3$ keV at 40–80 kpc, then decreases slowly beyond (Buote et al. 2003a). Similar temperature profiles are observed in many other groups and poor clusters (Sun et al. 2003; Loken et al. 2002). However, within about 30 kpc the X-ray spectrum is fitted better with two or more gas temperatures spanning the range $0.7\ \mathrm{keV} \lesssim kT \lesssim 1.3$ keV (Buote et al. 2003a). The low-temperature component at $kT \sim 0.7$ keV dominates the emission in this region but only occupies $\sim$0.5 of the volume out to 20 or 30 kpc. This suggests that the remaining volume is occupied by the hotter gas, which must be buoyant if it is in pressure equilibrium. This conclusion is directly supported by the pronounced spatial irregularities visible in the *Chandra* image of NGC 5044 (Buote et al. 2003a).

The iron abundance in NGC 5044 decreases from $\sim$1.3 solar near the center to $\sim$0.1 solar at $r = 150$ kpc and remains approximately uniform beyond (Buote et al. 2003b, 2004). The total mass of iron observed within 100 kpc is $1.2 \times 10^8\ M_\odot$, and α/Fe abundance ratios indicate that 70%–80% of this iron has been produced in SNeIa.

It is interesting to estimate the total mass of iron produced by SNeIa in the central elliptical galaxy over cosmic time,

$$M_{\mathrm{Fe}} = \int_{t_0}^{t_n} \mathrm{SNu}(t) \frac{1}{100} \frac{L_B}{10^{10}\ L_{B,\odot}} y_{\mathrm{Ia,Fe}} 10^9\, dt \qquad (1)$$

in $M_\odot$ (Mathews 1989), where t is in gigayears and $t_n = 13.7$ Gyr is the current age of the universe. The iron yield of each SNIa is $y_{\mathrm{Ia,Fe}} = 0.7\ M_\odot$. We assume an SNIa rate of

$$\mathrm{SNu}(t) = 0.16(t_n/t) \qquad (2)$$

in SNu (number per 100 yr per $10^{10}\ L_{B,\odot}$). The current SNIa rate in early-type galaxies is 0.16 ± 0.06 (Cappellaro et al. 1999). The SNu $\propto t^{-1}$ variation is consistent with the SNu $\propto t^{-1.2}$ variation observed by Pain et al. (2002) out to redshift 0.5, although the exponent 1.2 is uncertain. Suppose, for example, that most of the stars in NGC 5044 formed at cosmic time $t_f = 1.65$ Gyr (redshift $z = 4$), and a 1 Gyr delay preceded the first SNIa (Gal-Yam & Maoz 2004). In this case the integration above begins at time $t_0 = 2.65$ Gyr, corresponding to redshift $z \sim 2.5$. The integration predicts that $1.1 \times 10^8\ M_\odot$ of iron will have been been created by all SNeIa in the central elliptical galaxy NGC 5044.

It is remarkable that this estimate is comparable to the total mass of iron observed in the central iron peak out to 100 kpc, $M_{\rm Fe,obs} \approx 1.2 \times 10^8\ M_\odot$, suggesting that rather little SNIa iron is currently in the stars. At $r \gtrsim 100$ kpc the iron abundance in NGC 5044 plateaus at $z_{\rm Fe} \sim 0.1$ solar (Buote et al. 2004), so it is natural to assume that the background gas was pre-enriched everywhere by Type II supernovae in the early universe to $z_{\rm Fe} \approx 0.1$ solar. The total iron mass from this background within 100 kpc is only $0.2 \times 10^8\ M_\odot$, suggesting that 80% of the iron in the central peak is from SNeIa, which is consistent with X-ray spectra. While the uncertainty of past supernova rates certainly tempers our estimate of the total iron mass from SNeIa, its similarity to the observed mass has important implications for the global gasdynamics. Very recently, De Grandi et al. (2004) have shown that the mass of the excess iron surrounding cluster-centered elliptical galaxies correlates with their optical luminosity, just as we would expect from the integration above. Furthermore, most of the gas-phase iron in the central iron peaks of clusters and groups is observed to have an SNIa abundance signature within about 100 kpc of the central elliptical galaxy (De Grandi & Molendi 2001).

One possible explanation for the extended regions of iron enrichment is that the iron was created in SNeIa within the central elliptical galaxy, $r \sim R_e = 10$ kpc, but was subsequently distributed outward by merging events into the much larger region where it is observed today. Such mixing due to gas-phase mergers would need to be accompanied by an increased entropy if the iron-rich gas were to remain at a larger radius. If a merger radially mixes the gas without strong heating, after a dynamical time the gas will return to its original radius in the entropy structure and the original metallicity gradient will be restored. However, we expect that most of the shock energy dissipated (and entropy created) in mergers occurs closer to the virial radius, which is very much larger than the $r \lesssim 100$ kpc region enriched in iron. Central increases in gas-phase metallicity are only observed in the most relaxed groups and clusters; they are clearly an indication of an old system. If mixing due to mergers occurred long ago, not enough SNIa iron would be available to account for current observations.

In our previous gasdynamical studies including iron enrichment (reviewed in Mathews & Brighenti 2003b), we found that the radial distribution of gas-phase iron from both Type II and early-time SNeIa can extend well beyond the optical radius R_e of the central elliptical galaxy. This spatial spreading of the iron can result from early galactic winds if the central elliptical formed monolithically or from SNeIa in stars in the central elliptical galaxy located well beyond R_e, where both the stellar and gas densities are low. Nevertheless, these models cannot spread the iron to radii as large as $\sim$100 kpc, where it is typically observed.

In a recent paper (Buote et al. 2004), we have shown that very little of the gas-phase iron in the NGC 5044 group has been supplied by outflows from the large number of low-luminosity group member galaxies. The radial distribution of stellar mass in these noncentral group galaxies is approximately constant within the $\sim$100 kpc region, where the gas iron enrichment has a strong gradient. It is clear from our arguments in that paper that the mass of iron in the central peak within $\sim$100 kpc cannot be ascribed to starburst outflows or winds associated with other members of the NGC 5044 group.

It is difficult to escape the conclusion that a very large fraction of the iron in $r \lesssim 100$ kpc was produced by SNeIa associated with stars that are currently within the large central elliptical, but where were these stars when the iron was produced? Perhaps the extended iron enrichment occurred as the stars within the central elliptical galaxy were assembled. This seems unlikely, however, since the dynamical time for the assembly to occur, $\lesssim$1 Gyr, is very much less than the $\sim$10 Gyr time required to create $M_{\rm Fe} \approx 10^8\ M_\odot$ by SNeIa. Stars in galaxies undergoing dynamical friction spend most of their total lifetimes in the assembled elliptical galaxy, not in the assembly itself.

In this paper we consider an enrichment process in which iron from SNeIa in the central elliptical galaxy is heated by AGN activity and conveyed by buoyant transport to $r \lesssim$ 100 kpc in the surrounding hot gas, where it is currently observed. We show below that the AGN energetics required to centrally heat the gas are reasonable and consistent with other properties of galaxy groups containing hot gas. Furthermore, to store most or all of the iron from SNeIa over $\sim$10 Gyr, it is essential that very little of the iron-rich gas cools. This is possible, since the failure of cooling flows to cool is now widely accepted.

While we have used the NGC 5044 group in our discussion, the same argument could be applied to many other similar galaxy groups and poor clusters with $kT \sim 1$ keV: RGH 80 (Xue et al. 2004), NGC 507 (Kim & Fabbiano 2004), MKW 4 (O'Sullivan et al. 2003), and NGC 1399 (Buote 2000a, 2000b). In every case the hot gas surrounding the central elliptical has an extended region that can be fitted better with more than one local temperature and is enriched to $\langle z_{\rm Fe} \rangle \sim 0.5$ solar out to $\gtrsim$50 kpc by the products of SNeIa. The poor clusters M87 (Gastaldello & Molendi 2002) and Centaurus (Sanders & Fabian 2002) also have extended multitemperature, iron-rich regions surrounding the central elliptical galaxy.

3. CIRCULATION FLOW EQUATIONS

We consider a spherically symmetric cooling flow that flows in to some small radius r_h where it is heated. Plumes and bubbles of heated gas rise buoyantly upstream in the cooling flow until their entropy matches that of the inflowing gas, provided there is no energy exchange between the bubbles and the ambient flow. The rising gas bubbles displace the inflowing gas and reduce the volume through which it flows. Larger bubbles rise faster than smaller ones, since they experience less drag per unit mass (see eq. [13] of Mathews et al. 2003). The volume filling factor f available to the inflowing gas is difficult to estimate because it depends on the unknown bubble size distribution. Therefore, we use observations of NGC 5044 and RGH 80 as guides to parameterize $f(r)$ with the expression

$$f(r) = 1 - f_h e^{(r_h - r)/r_{2t}}, \tag{3}$$

where $f_h = 1 - f(r_h)$ and $r_{2t} = 30$ kpc is the maximum radius for which the X-ray spectrum shows two temperature components (Buote et al. 2003a). This form for $f(r)$ is also similar to the self-consistent filling factors we calculated for steady state circulation flows (Mathews et al. 2003). In reality, f may be a function of both radius and time, but we demonstrate below that the inflowing solutions are surprisingly insensitive to our choice for $f(r)$ and presumably also its time variation. The volume filled with inflowing gas in a shell of thickness dr is

$$dV = 4\pi r^2 f\, dr = A\, dr, \tag{4}$$

where A is the area available to the cooling inflow at radius r.

In this first time-dependent calculation of mass recirculation in cooling flows, we treat the central galaxy as a source of heating and iron enrichment at radius $r_h = 5$ kpc. This is a reasonable approximation, since the scale of the central galaxy is much less than the observed extent of ~50–100 kpc of the region of SNIa-enriched gas surrounding it. The equation of continuity for the cooling inflow is

$$\frac{\partial \rho}{\partial t} + \nabla \cdot \rho \boldsymbol{u} = \frac{dp}{dV}\left[M_*(\alpha_* + \alpha_{\rm SN}) + \left|\dot{M}_h\right|\right]. \quad (5)$$

The source term on the right-hand side represents the rate at which mass is recirculated per unit volume by rapidly buoyant bubbles arriving from the galactic core. Here

$$\dot{M}_h = 4\pi r_h^2 \rho_h u_h f(r_h) \quad (6)$$

is the rate at which mass arrives at the heating radius r_h, and $M_*(\alpha_* + \alpha_{\rm SN})$ is the (generally smaller) rate at which new mass is created in the central galaxy by stellar mass loss and SNeIa, respectively. The specific stellar mass-loss rate is

$$\alpha_*(t) = 4.7\times10^{-20}(t/t_n)^{-1.3}\ {\rm s}^{-1}, \quad (7)$$

where $t_n = 13.7$ Gyr is the current age of the universe. The mass-loss rate from SNeIa is

$$\alpha_{\rm SN} = 3.17\times10^{-20}{\rm SNu}(t)\left(\frac{M_{\rm SN}}{M_\odot}\right)\frac{1}{\Upsilon_B}\ {\rm s}^{-1}, \quad (8)$$

where Υ_B is the stellar mass to light ratio in the B band and $M_{\rm SN} = 1.4\ M_\odot$ is the mass ejected in each SNIa event.

The coefficient dp/dV in the source term for the equation of continuity is the normalized probability that mass heated at radius r_h will be transported to a remote volume dV in the flow. In our study of steady state circulation flows, we showed that the time for gas bubbles heated at r_h to move out to their final radius was $\lesssim 0.15$ of the flow time back to r_h. The time required for heated bubbles to reach their final radius is comparable to the dynamical time in the cluster potential, which is short compared to the cooling (or inflow) time; $t_{\rm dyn} \ll t_{\rm cool}$ is a defining characteristic of so-called cooling flows.

The normalization for the circulation probability is

$$\int_{r_h}^{r_e}\frac{dp}{dV}4\pi r^2 f\,dr = \int_{r_h}^{r_e}\frac{dp}{dr}\frac{4\pi r^2 f}{A}\,dr = \int_{r_h}^{r_e}\frac{dp}{dr}\,dr = 1, \quad (9)$$

where r_h and r_e are the minimum and maximum radii that define the region of circulation. This suggests a simple probability $p(r)$ that depends only on the radius, $dp/dr = A(dp/dV)$. For the mass redistribution we consider parameterized functions of the form

$$dp/dr = (dp/dr)_0\left(r/r_p\right)^n e^{-(r/r_p)^m} = (dp/dr)_0\xi^n e^{-\xi^m}, \quad (10)$$

where

$$\xi = r/r_p, \quad (11)$$

r_p is an adjustable scale factor, and m is either 1 or 2 but n can have any positive value. The normalization can be expressed in terms of incomplete gamma functions,

$$\left(\frac{dp}{dr}\right)_0 = \left\{\frac{r_p}{m}\left[\gamma\left(\frac{n+1}{m},\ \xi_e^m\right) - \gamma\left(\frac{n+1}{m},\ \xi_h^m\right)\right]\right\}^{-1}, \quad (12)$$

where $\xi_e = r_e/r_p$ and $\xi_h = r_h/r_p$. The probability distribution has a maximum at $r_m = r_p(n/m)^{1/m}$.

The density of iron requires a continuity equation of its own. If $n_{\rm H}$ is the proton number density in the hot gas, the density of hydrogen is $\rho_{\rm H} = n_{\rm H} m_p$, where m_p is the proton mass. The total density is

$$\rho = n_{\rm H} m_p \frac{5\mu}{4 - 3\mu} \equiv \rho_{\rm H}\phi, \quad (13)$$

where $\mu = 0.61$ is the mean molecular weight for full ionization and $\phi = 5\mu/(4 - 3\mu) = 1.41$ allows for the mass of helium. Since

$$z = \frac{\rho_z}{\rho_{\rm H}} = \phi\frac{\rho_z}{\rho}, \quad (14)$$

the density of element z (i.e., iron) is $\rho_z = \rho z/\phi$. The gas-dynamical evolution of the iron is most easily described by regarding the product ρz as a single variable,

$$\frac{\partial(\rho z)}{\partial t} + \nabla\cdot(\rho z)\boldsymbol{u} = \frac{dp}{dV}\left[M_*\left(\alpha_*\langle z_*\rangle + \alpha_{\rm SN}\frac{y_{Ia,{\rm Fe}}}{M_{\rm SN}}\phi\right) + \left|\dot{M}_h\right|z_h\right]. \quad (15)$$

Here $\langle z_*\rangle = 0.7 z_{{\rm Fe},\odot}$ is the adopted mean stellar iron abundance in the central galaxy (Rickes et al. 2004), and we take $z_{{\rm Fe},\odot} = 1.83\times10^{-3}$ as the solar abundance. Each SNIa remnant is assumed to contain $y_{Ia,{\rm Fe}} = 0.7\ M_\odot$ of iron. The production of iron by SNeIa is about 10 times greater than that due to stellar mass loss.

The equation of motion is

$$\frac{\partial u}{\partial t} + \nabla\cdot\boldsymbol{u} = -\frac{1}{\rho}\frac{dP}{dr} - g. \quad (16)$$

The gravitational acceleration $g = GM/r^2$ in the NGC 5044 group can be approximated with

$$g = \min\left(2.4319\times10^{-7}r_{\rm kpc}^{-0.75362},\ 4.762\times10^{-7}\right)\ {\rm cm\ s}^{-2}, \quad (17)$$

which is an excellent approximation for $0.1 < r_{\rm kpc} \lesssim 500$ to the mass profile discussed by Buote et al. (2004), i.e., a de Vaucouleurs stellar mass of $M_{*t} = 3.4\times10^{11}\ M_\odot$ with radius $R_e = 10.0$ kpc and a dark NFW halo (Navarro et al. 1997) of mass $4\times10^{13}\ M_\odot$ with concentration $c = 13$.

Although the temperature and density in rising bubbles should both match those in the surrounding gas when their entropies become equal, the mass added by recirculated gas in some remote volume dV must cause the local gas density to increase with time. If the density increases in some region of the flow, the increased radiative cooling there increases the density further. Eventually, the gas may cool catastrophically by runaway radiative losses. The dense, cooled gas then falls

into the gravitational potential and after time becomes supersonic, increasing $|\dot{M}_h|$ enormously.

To avoid these undesirable consequences, it is necessary to heat the inflowing gas as it moves past the rising bubbles. This heating can be due to $P\,dV$ work done by the expanding bubbles, the power expended by the drag force on the rising bubbles, and thermal mixing of some bubble gas with the local inflow. The thermal evolution of the bubbles may not be purely adiabatic. In this discussion we wish to avoid a detailed discussion of these complicated bubble-flow interactions and simply assume that a power $\epsilon_h L_h$ is transferred to the cooling flow, where L_h is a characteristic luminosity expended in heating gas at r_h and ϵ_h is a dimensionless factor of order unity. The magnitude of this heating luminosity is justified below. We also assume for simplicity that this distributed heating is transferred to the cooling flow with the same probability distribution dp/dV as the mass recirculation. Obviously, some very complicated bubble physics is subsumed with this assumption, some of which was discussed in our previous paper. However, by combining these detailed interactions into a single energy source term, we can explore new gasdynamical possibilities that must be verified by more detailed calculations in the future. The evolution of the energy density $e = P/(\gamma - 1)$, including this heating and radiation loss, is described by

$$\frac{\partial e}{\partial t} + \nabla\cdot\boldsymbol{u}e = -P\nabla\cdot\boldsymbol{u} - \frac{\rho^2}{m_p^2}\Lambda + \frac{3kT}{2\mu m_p}\frac{dp}{dV}\left[M_*(\alpha_* + \alpha_{\rm SN}) + \left|\dot{M}_h\right|\right] + \epsilon_h L_h \frac{dp}{dV}, \tag{18}$$

where ϵ_h is of order unity and $\Lambda(T, z)$ is the usual coefficient for optically thin radiative cooling (Sutherland & Dopita 1993). The terms on the right-hand side respectively represent compressive heating, cooling by radiative losses, addition of thermal energy density associated with the (nonheating) mass deposition, and genuine heating provided by the mass deposition. When $\epsilon_h = 0$ the recirculated mass is assumed not to heat or cool the gas, so the specific thermal energy $3kT/2\mu m_p$ contributed by the recirculated gas is identical to that of the local gas. Consequently, the energy density equation must have a source term analogous to that in equation (5). This third term on the right-hand side of equation (18) has little effect on the solutions.

While the spatial distribution dp/dV of the bubble heating term $\epsilon_h L_h(dp/dV)$ need not be identical to that of the recirculated mass, it is the simplest assumption that involves the fewest additional parameters and seems appropriate for this initial study of time-dependent circulation. The power expended in heating the gas at r_h is

$$L_h = \left[M_*(\alpha_* + \alpha_{\rm SN}) + \left|\dot{M}_h\right|\right]\frac{3kT_h}{2\mu m_p}\langle h\rangle, \tag{19}$$

where $T_h = T(r_h)$ is the temperature of the inflowing gas at r_h and $\langle h\rangle$ is a dimensionless mean heating factor required to recirculate the gas.

The mean heating factor $\langle h\rangle$ can be estimated by examining how the incoming gas is heated at r_h and assuming adiabatic bubble evolution. Bubbles are formed at r_h with temperature

$$T_{b,h} = hT_h \tag{20}$$

where $T_h = T(r_h)$ is the cooling flow temperature at the heating radius. [Virialized gas lost from stars in the central galaxy is also assumed to have a preheating temperature $\sim T_h$; in general, $|\dot{M}_h|$ is considerably larger than $M_*(\alpha_* + \alpha_{\rm SN})$.] The bubbles are always in pressure balance with the surrounding gas,

$$T_b = \rho T/\rho_b, \tag{21}$$

and so

$$\rho_{b,h} = \rho_h/h. \tag{22}$$

As bubbles move out from r_h, their entropy is assumed to be constant:

$$T_b = T_{b,h}\left(\frac{\rho_b}{\rho_{b,h}}\right)^{\gamma-1} = T_h h^{\gamma}\left(\frac{\rho_b}{\rho_h}\right)^{\gamma-1}. \tag{23}$$

Some deviation from constant entropy is expected if the bubbles radiate or if they lose mechanical energy in heating the surrounding gas, so our adiabatic assumption is a limiting case. Eliminating T_b from the equations above gives an equation for the bubble density at $r > r_h$,

$$\frac{\rho_b}{\rho_h} = \frac{1}{h}\left(\frac{\rho}{\rho_h}\frac{T}{T_h}\right)^{1/\gamma}, \tag{24}$$

and, if the entropy is conserved,

$$\frac{T_b}{T_h} = h\left(\frac{\rho}{\rho_h}\frac{T}{T_h}\right)^{(\gamma-1)/\gamma}. \tag{25}$$

Adiabatically rising bubbles expand and cool. By examination of the last two equations above, as outflowing bubbles of constant specific entropy approach the radius in the flow at which the flow entropy matches that of the bubbles, $S_b \rightarrow S(r)$, the densities and temperatures also become equal, i.e., $\rho_b \rightarrow \rho$ and $T_b \rightarrow T$. The specific thermal energy of gas adiabatically transported in this manner to distant regions of the flow is identical to that in the surrounding gas, and no heating occurs in this idealized approximation. We see below, however, that the increase in gas mass in the flow due to the deposition of outflowing gas actually results in a higher gas density, which is further increased by (nonadiabatic) radiative cooling. Alternatively, if bubbles of hot gas thermally merge with their environment at some smaller radius where $S_b > S(r)$, the surrounding flow will be heated.

From the last two equations above, the entropy $S = T/\rho^{\gamma-1}$ of heated bubbles at r_h is

$$S_b = h^{\gamma}S_h, \tag{26}$$

where $S_h = S(r_h)$. This last equation associates the heating parameter h with a unique bubble entropy and therefore with a unique radius r in the cooling flow, assuming that the entropy of the cooling inflow increases monotonically with radius and that the bubbles remain adiabatic. In NGC 5044 and other similar cooling flows, as well as for the circulation flows considered here, $S \propto r$ is a good approximation, so

$$h = \left(\frac{S}{S_h}\right)^{3/5} = \left(\frac{r}{r_h}\right)^{3/5} \text{ or } r = r_h h^{5/3}, \tag{27}$$

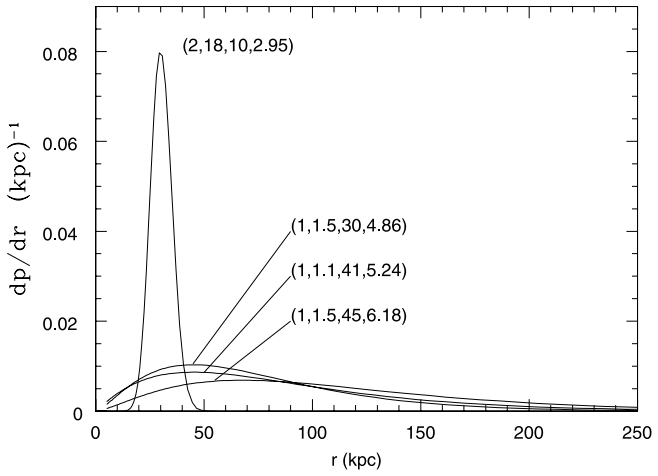

FIG. 1.—Normalized mass redistribution probability functions dp/dr, each labeled with (m, n, $r_{p,\mathrm{kpc}}$, $\langle h \rangle$).

where we assume $\gamma = 5/3$. The mean heating factor is approximately

$$\langle h \rangle = \int_{r_h}^{r_e} h \frac{dp}{dV} 4\pi r^2 \, dr = \frac{1}{b(n,\ m)} \int_{\xi_h}^{\xi_e} e^{-\xi^m} \left(\frac{\xi}{\xi_h}\right)^{3/5} \xi^n \, d\xi$$
$$= \frac{1}{b(n,\ m)\xi_h^{3/5}} \left[\gamma\left(\frac{n+1.6}{m},\ \xi_e^m\right) - \gamma\left(\frac{n+1.6}{m},\ \xi_h^m\right)\right], \quad (28)$$

where $b(n,\ m)$ is the quantity in square brackets in equation (12). Figure 1 shows a sample of normalized circulation probabilities dp/dr that we consider below, with each curve labeled with the parameters m, n, $r_{p,\mathrm{kpc}}$, and the mean heating factor $\langle h \rangle$.

In our previous paper on steady state circulation flows, we considered in detail the dynamics of buoyant bubbles, including the exchange of momentum between the cooling inflow and the counterstreaming heated bubbles (Mathews et al. 2003). We showed that this momentum exchange is not particularly important for a wide range of bubble sizes. In addition, we discussed in detail the contribution of the heated gas to the overall X-ray emission. The X-ray emission from rising bubbles is small but observable, but emission from the hottest gas, which ends up at the largest radii, is necessarily the lowest because of its low density. In the standard single-temperature interpretation of the X-ray emission from NGC 5044 and other similar flows, the observed temperature is dominated by that of the dense inflowing gas, as we have shown in our previous paper on circulation flows (Mathews et al. 2003). Finally, in this earlier paper we discussed in detail the various heating processes by which the rising bubbles can share energy with the ambient gas. We see below that energy exchange between gas flowing in opposite directions is critical to the success of time-dependent circulation flows.

4. RESULTS

4.1. *Pure Cooling Flows*

Gasdynamical solutions are found by solving equations (5), (15), (16), and (18) in spherical symmetry using a one-dimensional ZEUS-like Eulerian code (Stone & Norman 1992). We employ a computational grid of 100 logarithmically increasing zones between $r_h = 5$ kpc and $r_e = 500$ kpc in which the first zone is 215 pc in width. Outflow boundary conditions are imposed at r_h, and the boundary at r_e is fixed and reflecting, since it is far beyond the cooling radius ($\sim$60 kpc), where the radial flow is negligible.

Our first objective is to establish a dynamically relaxed cooling flow without mass recirculation, i.e., $dp/dV = 0$. This flow can serve as a smooth starting point for flows with circulation. Solutions with $dp/dV = 0$ also allow us to explore the effect that various filling factors $f(r)$ have on the flow. The initial conditions for these pure cooling (and noncirculating) flows are the temperature and density profiles observed in NGC 5044 (Buote et al. 2003a). The gas is initially at rest. These initial profiles are shown with dotted lines in Figure 2. Three cooling flows are calculated for 10^{10} yr between r_h and r_e for three fixed filling factors of $f(r_h) = 0.3$, 0.5 and 1, but all with $r_{2t} = 30$ kpc (see eq. [3]).

After 10 Gyr the computed gas density and temperature profiles, shown with solid lines in Figure 2, remain in reasonably good agreement with the profiles observed in NGC 5044 today, shown with dotted lines. While this is reassuring, it has no particular significance, since there is no reason to expect that the profiles observed today should persist over such a long time, particularly since our flows include no heating. Some modest heating does seem to be required for $r \lesssim 100$ kpc, where the computed temperature profiles are $\sim$0.2–0.3 keV below those observed. Gas beyond about 100 kpc does not change appreciably during the entire calculation, although information moves at the sound speed from r_h to r_e in only 0.95 Gyr. Both observed and computed temperature profiles $T(r)$ exhibit maxima well beyond the optical half-light radius, $R_e = 10$ kpc, of the central elliptical galaxy. This thermal feature, which is observed in hot gas on all scales from galaxies to rich clusters, is a characteristic signature of cooling by radiative losses. The overall approximate agreement of our simple cooling flows with NGC 5044 indicates that, to a first approximation, the X-ray emission from this group is dominated by inflowing gas that resembles a conventional cooling flow.

The observed entropy, pressure, and density profiles plotted in Figure 2 with dotted lines have been interpreted assuming that the filling factor is unity. However, the computed solid line curves in Figure 2 are the actual variables in the gas flowing for each assumed $f(r)$. Therefore, to compare the computed flows (*solid lines*) in Figure 2 with observations, the computed density profiles would need to be adjusted downward by $n_e \rightarrow f(r)^{1/2} n_e$ and the entropy upward by $S(r) \rightarrow f(r)^{-1/3} S(r)$. Both these adjustments tend to bring the solid curves into better agreement with the observations at small radii.

The most useful result in Figure 2 is the insensitivity of the inflowing gas density and temperature profiles to large variations in the filling factor $f(r)$. To the accuracy that we require for our goals here, the computed gas profiles are identical for all three $f(r)$. The similarity of flows with different filling factors is particularly advantageous because of the difficulty in determining the filling factor either from first principles or from very detailed numerical calculations; fortunately, $f(r)$ can be found from observations. In our study of steady state circulation flows, we were able to determine the filling factor for the return flow in a self-consistent manner only if all bubbles were assumed to have the same mass (Mathews et al. 2003). However, in view of the insensitivity to $f(r)$, none of the conclusions that we reach below depends strongly on the particular filling factor $f(r)$ chosen or its possible variation with time, provided that it does not deviate radically from the three

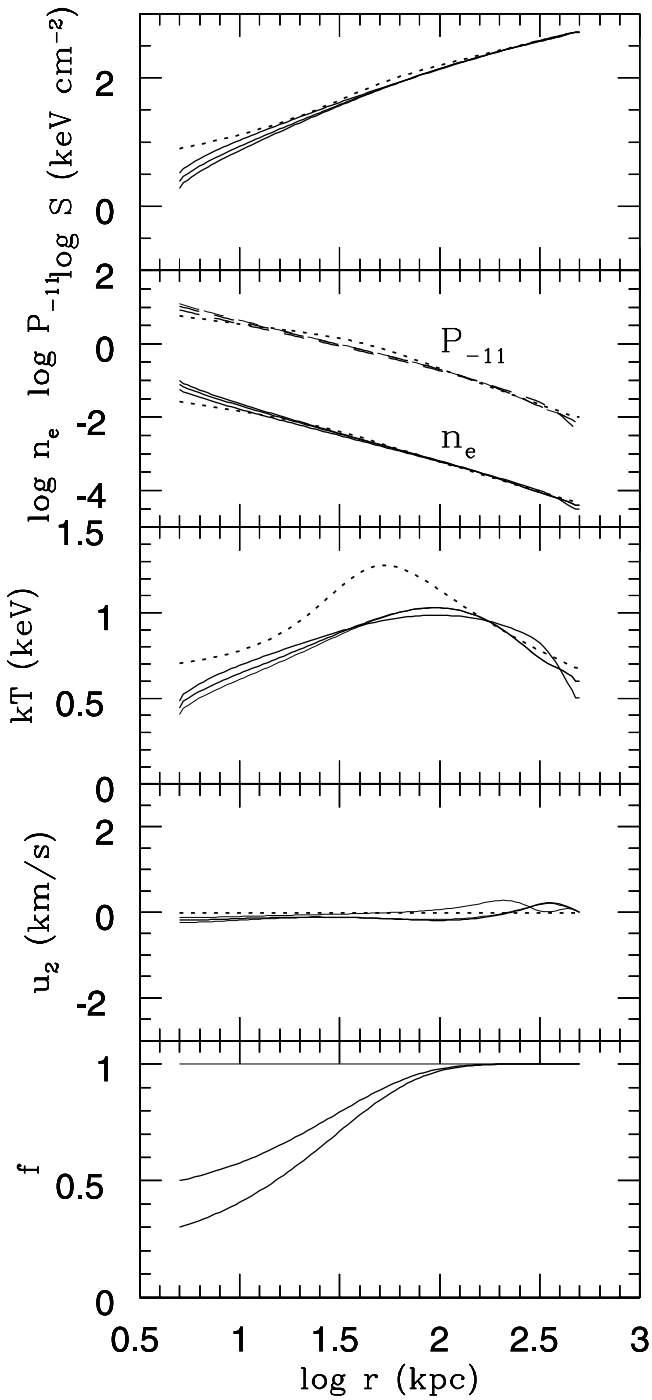

FIG. 2.—Pure cooling flows (*solid lines*) after evolving for 10 Gyr with three different filling factor profiles $f(r)$. The dotted lines show the density and temperature profiles observed in NGC 5044 that serve as initial conditions for the computed profiles; the dotted line pressure and entropy profiles are derived from the observations. The filling factors correspond to $f(r_h) = 0.3$, 0.5, and 1.0, all with $r_{2t} = 30$ kpc. In descending order from the top, the panels show profiles for the gas entropy $S = kT/n_e^{2/3}$, the gas density n_e (*solid lines*) and pressure P (*dashed lines*) in units of 10^{-11} dynes, the gas temperature kT, the gas velocity $u_2 = u/(100 \text{ km s}^{-1})$, and the flow filling factor f. The low-amplitude velocity profiles with $f(r_h) = 0.3$ and $f_h = 0.5$ are fortuitously identical.

$f(r)$ illustrated in Figure 2 that bracket the known observations of galaxy groups. Therefore, in the remaining flows discussed below, we adopt a fixed filling factor with parameters $f_h = 0.5$ and $r_{2t} = 30$ kpc.

4.2. *Nonheated Cooling Flows with Mass Circulation*

As discussed earlier, we consider the possibility that most or all of the gas that flows into the central galaxy, as well as gas expelled from evolving stars, is heated and buoyantly transported, with its iron, into the large volume of the surrounding hot gas. Heating near r_h is assumed to be continuous and isotropic, creating bubbles that flow out in every direction. In this initial study of time-dependent circulation flows, we exploit the defining property of cooling flows that the dynamical time is much less than the cooling time. Indeed, as we showed in Mathews et al. (2003), the dynamical time for heated gas to rise buoyantly is much less than the radiative cooling time that governs the incoming flow.

In this section we describe circulation flows in which bubbles of gas heated near radius $r_h = 5$ kpc float outward without heating the incoming flow. In view of the variety of complicated ways that rising bubbles can heat the inflowing gas, it is useful to consider flows with no heating as a useful intermediate step toward more realistic flows. These idealized bubbles rise adiabatically to their final radius and deposit gas into the cooling flow at a radius where the entropy and specific thermal energy of the bubble are identical to those in the ambient flow.

Nonheated circulation flows can be studied by allowing recirculation of mass, $dp/dV \neq 0$, but not heat energy, i.e., ϵ_h is set to zero in equation (18) so there is no distributed energy source. Each flow (and those discussed subsequently) begins at cosmic time $t = 2.65$ Gyr, corresponding to a redshift of 2.5, with initial conditions taken from the fully relaxed $f = 1$ solution in Figure 2. The spatial evolution of the iron abundance $z_{\rm Fe}(r, t)$ is also followed. We find that such nonheated flows cool catastrophically and deviate strongly from the observations. Such cooling is not desired in our solutions, since we wish to retain all of the SNIa iron in the hot gas as the observations suggest.

If the mass circulation pattern dp/dV is too concentrated near some radius r_m, the increased gas density there leads to rapid radiative losses and eventual cooling. Such a case is illustrated in Figure 3, in which the recirculation and heating parameters for dp/dV are $(m,\ n,\ r_{p,\rm kpc},\ \epsilon_h) = (2,\ 18,\ 10,\ 0)$. For this dp/dV the recirculated mass is deposited in an annulus $\sim$10 kpc wide located at $\sim$30 kpc. As it grows in mass, this shell cools and settles inward in the gravitational potential. At time 3.6 Gyr, as shown in Figure 3, some gas has cooled to $T \lesssim 10^5$ K, and the flow does not subsequently recover from this state.

Therefore, the commonly held notion that bubbles of heated gas rise adiabatically to some radius where their entropy S_b matches that of the local cooling flow S cannot be sustained because the local entropy of the flow is reduced as recirculated mass is introduced. Even if the mass in an annular shell increases at constant temperature, the gas density increases and local radiative losses are stimulated; both processes decrease the local gas entropy. This is an important consideration that leads to the failure of all models described in this section. Our discussion in § 3 relating the heating factor h to a unique radius r must necessarily be viewed as a semiquantitative idealization.

The iron abundance in Figure 3 is distributed within a region between the current location of the dense shell and the

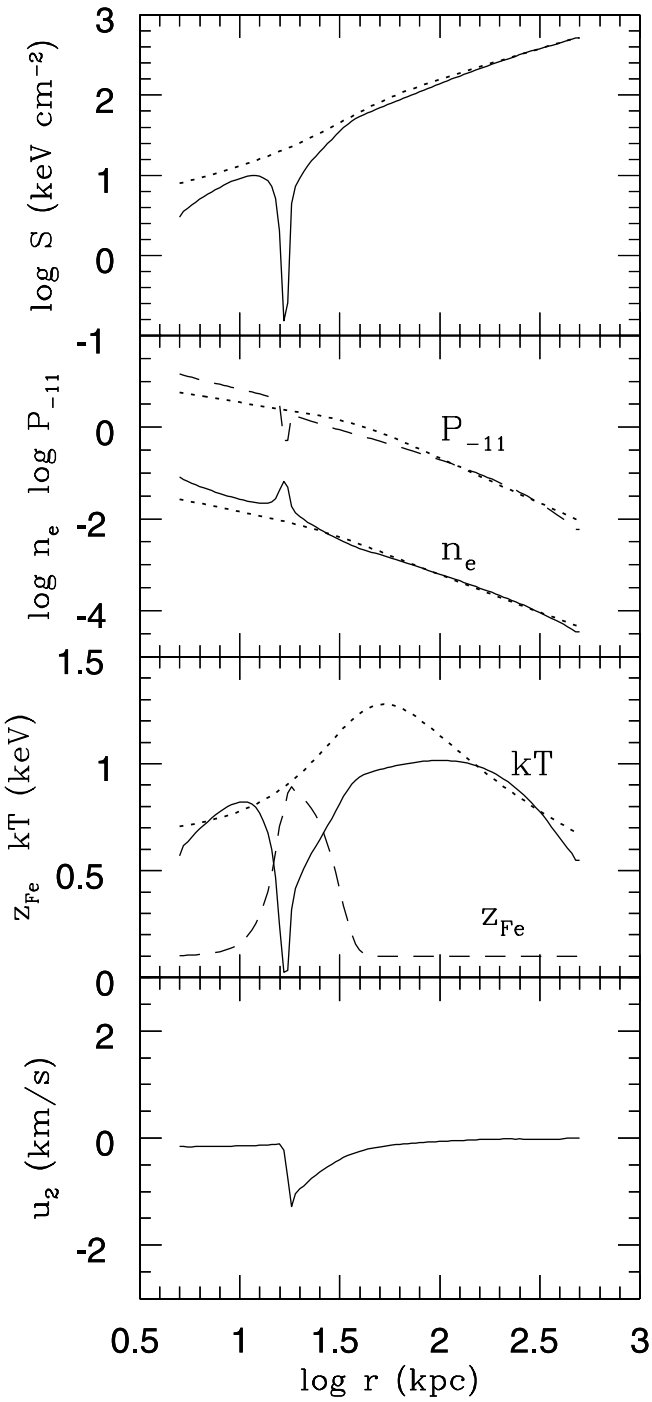

FIG. 3.—Nonheated circulation flow (*solid lines*) in which the mass recirculation probability dp/dV is concentrated near $r_m = 30$ kpc, $(m,\ n,\ r_{p,\mathrm{kpc}},\ \epsilon_h) = (2,\ 18,\ 10,\ 0)$. The flow began at cosmic time $t = 2.65$ Gyr and is shown at $t = 3.6$ Gyr, when severe cooling occurs. The dashed lines show the gas pressure and the iron abundance in solar units. The dotted lines show the observed $n_e(r)$ and $T(r)$ profiles for NGC 5044.

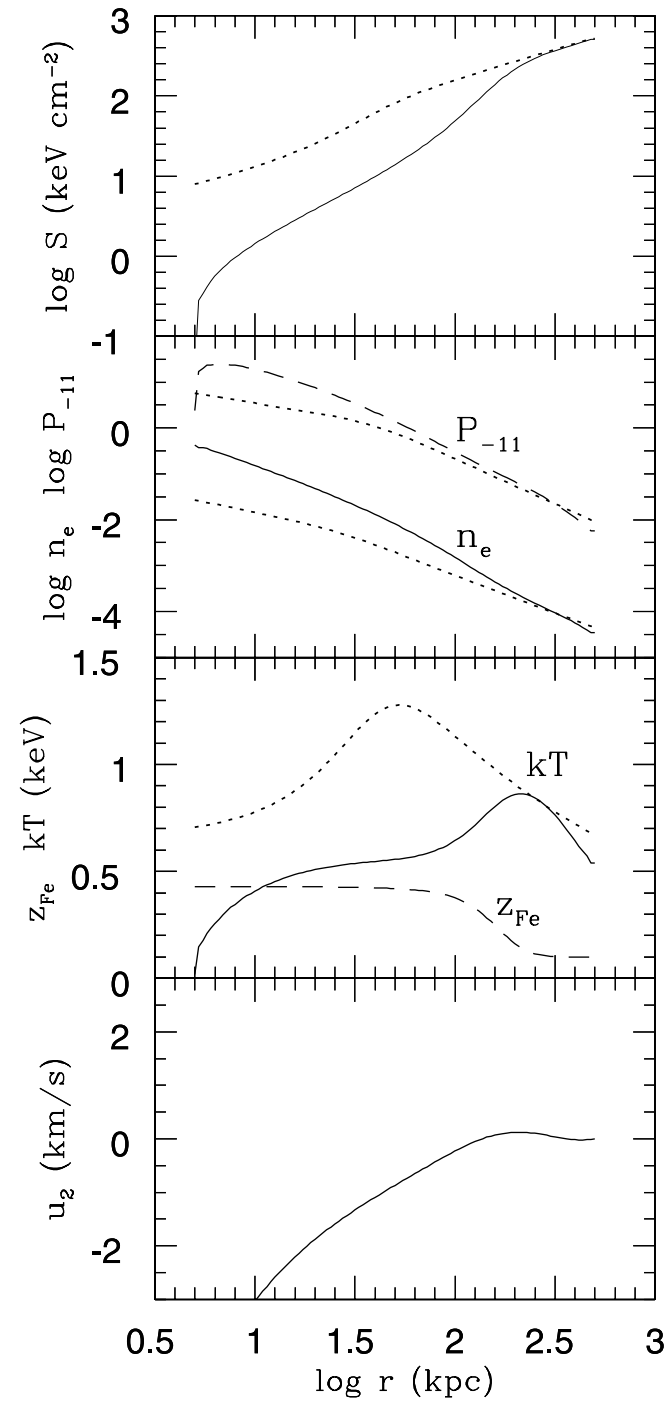

FIG. 4.—Nonheated circulation flow (*solid lines*) in which the mass recirculation probability dp/dV is a broad function extending out to several hundred kpc, $(m,\ n,\ r_{p,\mathrm{kpc}},\ \epsilon_h) = (1,\ 1.5,\ 30,\ 0)$. The flow is shown at time $t = 8.0$ Gyr, when catastrophic cooling occurred at the inner radius. The dashed lines show the gas pressure and the iron abundance in solar units. The dotted lines show the observed $n_e(r)$ and $T(r)$ profiles for NGC 5044.

somewhat larger radius r_m at which dp/dV has a maximum. A similar localized cooling can develop if the mass recirculation is more evenly distributed just between r_h and some radius $r_{\max}$ less than the cooling radius. If the mass deposition decreases sharply at $r_{\max}$, the cooling inflow from $r > r_{\max}$ can be locally decelerated and compressed near $r_{\max}$. This sort of flow, not illustrated here, can result in radiative cooling to low temperatures in a gaseous shell. Such compressive cooling was anticipated in our earlier work on steady circulation flows and resembles the cooling galactic drips discussed by Mathews (1997).

Circulation flows without distributed heating ($\epsilon_h = 0$) also fail, even if the mass redistribution dp/dV is very broad. Such a flow, with parameters $(m,\ n,\ r_{p,\mathrm{kpc}},\ \epsilon_h) = (1,\ 1.5,\ 30,\ 0)$, is illustrated in Figure 4 at time 8.0 Gyr, when the flow has cooled catastrophically near $r_h = 5$ kpc. In this flow the entropy

$S = kT/n_e^{2/3}$ out to $\sim$160 kpc has been dramatically reduced because of radiative losses associated with the increased density. As the density increases, the gas pressure gradient must become more negative to balance the gravitational potential, causing the gas pressure at small radii to increase. The gas pressure actually develops a maximum just beyond r_h within which gas is forced inward. The entire gas flow within $\sim$160 kpc approaches that of free fall, and the mass flux at r_h, $|\dot{M}_h|$, becomes very large. The high inflow velocity and the rapid recirculation of gas from r_h to larger radii cause the iron abundance to be low and flat-topped, as seen in Figure 4.

4.3. *Circulation Flows with Heating*

Fortunately, catastrophic cooling is easily eliminated by introducing a distributed heating term in the energy equation, $\epsilon_h > 0$. For simplicity, we consider heating that is distributed over the flow with the same normalized probability distribution dp/dV that describes the mass circulation. Even with this constraint, many circulation flow models are in satisfactory agreement with observation.

The time-dependent flows we describe here are often in a quasi–steady state, stable over long periods of time, so it is interesting to consider how the interbubble gas is heated by counterstreaming bubbles in the steady state limit. As a matter of principle, an ensemble of outflowing and expanding bubbles does not heat the surrounding gas by performing $P\,dV$ work provided that conditions are approximately steady state (Mathews et al. 2003). Certainly, a single bubble that suddenly appears and rises into an atmosphere of hot gas displaces its volume in the ambient gas at every radius and moves some ambient gas higher in the gravitational potential. In this case $P\,dV$ work is done as the cloud expands and moves outward. However, a single buoyant cloud is not a steady state phenomenon; it is inherently time dependent. An approximate steady state is possible only if many clouds are flowing through each shell of volume $dV = 4\pi r^2 dr$ at any time. In this case the volume filled with rising bubbles $(1 - f)\,dV$ is nearly constant; as bubbles exit from the surface at $r + dr$, new ones appear at r, approximately conserving the number and total volume of bubbles. Individual bubbles expand adiabatically as they move from r to $r + dr$, and their internal energy decreases accordingly. However, this expansion does not continuously heat the interbubble gas since, in the strict steady state sense, this work was already done by similar bubbles at an infinite time in the past. Since the volume of the interbubble gas does not change in steady flow, $f\,dV/dt = 0$, and the surrounding gas experiences no continuous $P\,dV/dt$ heating. Instead, as bubbles move through dV, the ambient cooling flow gas is subsonically rearranged transversely along equipotential surfaces, conserving its total volume. However, some work is done against viscous forces during this rearrangement. As a result, each bubble experiences a drag force as it moves upstream through the interbubble gas. Work done against viscous drag is a continuous source of spatially distributed heating in the surrounding gas.

Figure 5 illustrates two heated circulation flows that evolved without catastrophic radiative cooling from 2.65 to 13.7 Gyr and that are in reasonable agreement with the observed properties of NGC 5044 and other similar X-ray–luminous groups. The final temperature and iron abundance profiles of a flow described with circulation parameters $(m,\ n,\ r_{p,\mathrm{kpc}},\ \epsilon_h) = (1,\ 1.5,\ 45,\ 1.6)$ are shown as thin solid and thin dashed lines in Figure 5. The parameters for this flow were chosen to fit the observed temperature profile of

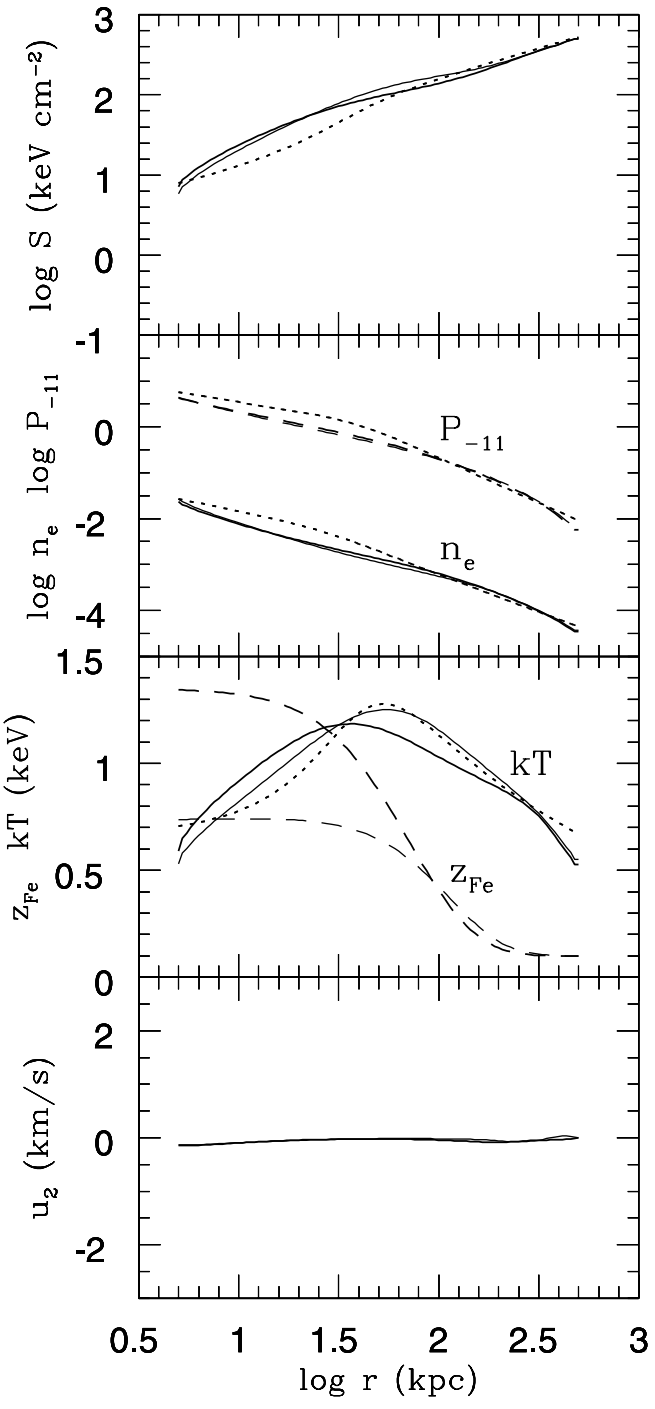

FIG. 5.—Two heated circulation flows (*solid lines*) with slightly different mass recirculation probabilities dp/dV that give good agreement at time $t = 13.7$ Gyr with the iron abundance and temperature profiles observed in NGC 5044. The dashed lines show the gas pressure and the iron abundance in solar units. Thick and thin lines correspond to probabilities dp/dV defined by $(m,\ n,\ r_{p,\mathrm{kpc}},\ \epsilon_h) = (1,\ 1.1,\ 41,\ 1.9)$ and $(1,\ 1.5,\ 45,\ 1.6)$, respectively. The dotted lines show the observed $n_e(r)$ and $T(r)$ profiles for NGC 5044.

NGC 5044, but the iron abundance does not exceed about 0.7 solar, somewhat lower than that observed in this group (Buote et al. 2003b). The iron abundance observed in NGC 5044, which rises to $\gtrsim$1 solar at $r \lesssim 20$ kpc, is better fitted with the circulation flow $(m,\ n,\ r_{p,\mathrm{kpc}},\ \epsilon_h) = (1,\ 1.1,\ 41,\ 1.9)$, which is shown with thick solid and thick dashed lines in Figure 5. Because of the slightly larger heating $\epsilon_h = 1.9$ in this flow, the inflow velocities are lower as the gas approaches r_h, and the

iron abundance there is correspondingly larger. For both flows in Figure 5 the total mass of iron within 100 kpc is about $10^8\ M_\odot$, since we use the same SNIa rate as in equations (1) and (2).

Evidently, if we relaxed our constraint that the recirculation distributions dp/dV of mass and heat energy be identical and allowed them to vary with time, it would be possible to match both the abundance and gas temperature profiles for any observed group. The density, pressure, flow velocity, and entropy profiles for the two flows shown in Figure 5 are acceptable fits to the NGC 5044 observations. Indeed, we find similar flows with a range of parameters (m, n, $r_{p,\mathrm{kpc}}$, ϵ_h), indicating that our results are robust.

It is particularly significant that the computed temperature profiles $T(r)$ in Figure 5 have maxima and positive gradients $dT/dr > 0$ at small r. In our previous paper on circulation flows (Mathews et al. 2003), we showed that the X-ray emission from hotter buoyant clouds of much lower density does not significantly alter the single-phase temperature profile established by the denser inflowing gas. However, in the diffusely heated one-dimensional and two-dimensional cooling flows that we previously solved with numerical hydrocodes, we invariably found monotonically decreasing temperatures $dT/dr < 0$ in the centrally heated region (e.g., Brighenti & Mathews 2002). In those calculations we heated all the gas throughout a volume near the center of the flow, including gas at all densities, and our specific objective was not to create or follow bubbles in the heated region. Some larger buoyant bubbles flowed out from the heated region, but they were not resolved in part because of spurious numerical diffusion. We avoid numerical diffusion here by assigning a fraction $1 - f(r)$ of the volume to the buoyantly outflowing heated gas. But the outwardly increasing temperature near the center in Figure 5 is made possible only by the combined influence of the redistribution of heated mass and the cooling inflow.

The profiles shown in Figure 5 are not momentary transients that happen to be similar to the observations at time $t_n = 13.7$ Gyr. While these flows are fully time dependent, the gas density and temperature profiles remain highly stable during the last $\sim$6 Gyr of the calculations. These flows are therefore quasi-steady, and the main secular change is the slowly increasing iron abundance $z_{\mathrm{Fe}}(r)$. Finally, we emphasize that the circulation of mass that we describe here cannot be viewed as normal convection, in which the entropy profile is flat, the temperature fluctuations are small, and the temperature gradient is negative.

Figure 6 shows the time variation of several global parameters for the two circulation flows illustrated in Figure 5. The mass flow rate $|\dot{M}(r_h)|$ at r_h, the stellar mass-loss rate $\dot{M}_*$, and the approximate power expended in heating the gas at r_h, $\epsilon_h L_h$, in units of 10^{42} ergs s^{-1}, all slowly decrease with time. The current heating luminosity $\epsilon_h L_h = 3.5 \times 10^{42}$ ergs s^{-1} is comparable to the X-ray luminosity of NGC 5044, $L_{\mathrm{X}} = 5.5 \times 10^{42}$ ergs s^{-1}, and this is expected in order to maintain the flow without radiative cooling to low temperatures. This level of heating $\epsilon_h L_h$ corresponds to a rather low-level AGN, which is consistent with other observations of NGC 5044.

In Mathews et al. (2003) we showed that the heating of the cooling inflow by bubbles due to work done against drag forces and $P\,dV$ expansion (if applicable) are comparable. We now estimate the collective heating by bubbles in NGC 5044 due to drag interactions. Assuming that the bubble velocity u_b is much greater than that of the cooling inflow, the terminal

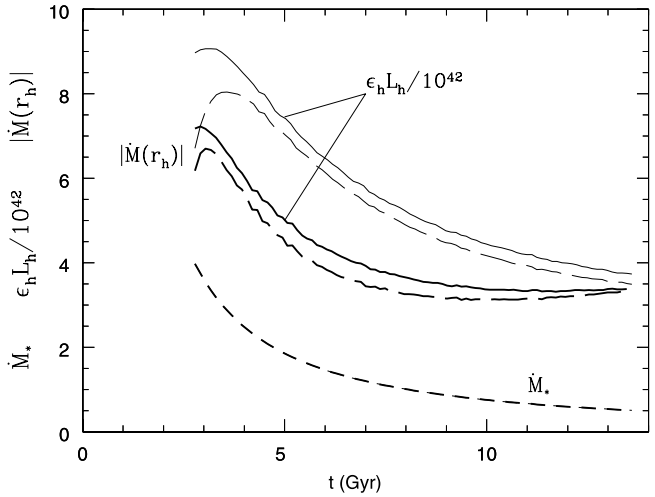

FIG. 6.—Variation with time of several properties of heated flows with parameters (m, n, $r_{p,\mathrm{kpc}}$, ϵ_h) = (1, 1.1, 41, 1.9) (*thin lines*) and (1, 1.5, 45, 1.6) (*thick lines*). Shown are the mass inflow rate at r_h, $|\dot{M}(r_h)|$, in $M_\odot$ yr^{-1} (*long-dashed lines*), the total stellar mass-loss rate $\dot{M}_*$ in $M_\odot$ yr^{-1} in the central elliptical galaxy (*short-dashed lines*), and the heating luminosity $\epsilon_h L_h$ in units of 10^{42} ergs s^{-1} (*solid lines*).

velocity is $u_b \approx (4gr_b\alpha/3\delta)^{1/2}$, where $\delta \sim 0.5$ is the dimensionless drag coefficient and $\alpha = 1 - (\rho_b/\rho)$. The rate at which energy is lost from a single bubble of radius r_b is then $l_d = \delta\rho u_b^3 \pi r_b^2$. The space density of bubbles is $n_b \approx 3(1-f)/4\pi r_b^3$. The heating rate due to all bubbles is

$$L_d \approx \int 3(1-f)\delta(\rho/r_b)u_b^3 \pi r^2\, dr \approx 9 \times 10^{42}\ \mathrm{ergs\ s^{-1}},$$

assuming $\langle h \rangle = 5$ and coherent bubbles of radius 0.5 kpc formed at $r_h = 5$ kpc, and taking $\rho(r)$ as the density profile observed in NGC 5044. The bubbles are assumed to be in pressure equilibrium, and the integration extends from r_h to the radius of equal entropy where $S_b = S$. In spite of the obviously approximate nature of this estimate, it is within a factor of 2 or 3 of the heating luminosities $\epsilon_h L_h$ required for the flows illustrated in Figure 5. Therefore, the amount of distributed heating we require for successful flows is comparable to that expected from bubble-flow interactions.

In our models the heating is continuous, but it may be possible to create similar circulation flows with intermittent heating near the center. It is likely, however, that the intermittency, if it exists, has a rather short period or duty cycle. The dynamical outflow time for bubbles of size r_b at radius r is $t_b \approx r/u_b$. For bubbles of radius $r_b = r/5$ at $r = 10$ kpc, $u_b \approx 260$ km s^{-1}, and the bubble rise time $t_b \approx 3 \times 10^7$ yr is rather short. If the gas is heated periodically, the period would have to be less than this and may in fact be very much less. Hot bubbles appear in the *Chandra* image of NGC 5044 well within 10 kpc from the center, and the X-ray image of NGC 5044 is similar to those of other elliptical galaxies with comparable L_B. If mass circulation is a common feature of all flows of this type, the implication is that there are no truly quiescent supermassive black holes.

Finally, we note that the heating due to SNeIa is small compared to L_h. For example, at time $t = t_n$ the total SNIa heating luminosity is $L_{\mathrm{Ia}} \approx (M_{*t}/M_{\mathrm{SN}})E_{\mathrm{SN}}\alpha_{\mathrm{SN}}$ ergs s^{-1}, where $E_{\mathrm{SN}} = 10^{51}$ ergs is released with each supernova. Evaluating at t_n, we find $L_{\mathrm{Ia}} \approx 2.3 \times 10^{41}$ ergs s^{-1}, which is very much less

than $\epsilon_h L_h$. For simplicity we have ignored supernova heating in equation (18).

4.4. *Central Iron Abundance Minimum*

One of the strangest features occasionally observed in cooling flows is a central minimum in the iron abundance (Johnstone et al. 2002; Sanders & Fabian 2002; Schmidt et al. 2002; Blanton et al. 2003; Dupke & White 2003). When present, these minima typically lie within the central ~10–50 kpc of the flows, i.e., where conditions are dominated by the central elliptical galaxy. Such minima—or a central flattening in $z_{\rm Fe}(r)$, which is even more common—would not be expected in conventional cooling flows, since the local frequency of iron-producing SNeIa should increase with the stellar density toward the very center of the flow. (The stellar density is more centrally peaked than the gas density.) Efforts to understand the central dips in the iron abundance in terms of differential cooling of abundance inhomogeneities have been discussed by Morris & Fabian (2003).

In the circulation flows described here it is possible to produce small central iron abundance minima if the redistribution probability dp/dV varies with time. For example, a small central dip in the iron abundance results if the iron (and mass) deposition dp/dV is concentrated near 40–50 kpc, just preceding the flow time for gas in this region to return to r_h by the current time $t = 13.7$ Gyr. Central regions with very low iron abundance are difficult to form in circulation flows because (1) the cooling inflow necessary to explain the observed gas temperature profile continuously recirculates iron-enriched gas within ~50 kpc and (2) since most of the SNIa iron is produced at early times, relatively little iron is available during the last cooling inflow time to create a strong reversal in the iron abundance profile. For these same reasons, central iron deficiencies are not easy to produce by allowing the iron mass and energy redistribution probabilities dp/dV to differ. Nevertheless, because of the continuous radial recirculation, it is quite natural for the central gas iron abundance in circulation flows to become rather constant within ~30 kpc, where the SNIa-producing stars are very strongly peaked. Similar flat or slowly varying iron abundance cores are commonly observed in many groups and clusters.

5. ADDITIONAL REMARKS

Although the heated flows we describe here are generally successful, much additional work will be necessary before they can be fully accepted. We have not identified the physical mechanism(s) that heat the gas near the center, but they are likely to be associated with the central black hole. These heating processes may be related to the common difficulty in observing hot gas in close proximity to the central black hole, constraining the accretion rate to less than 10% of the Bondi rate (Loewenstein et al. 2001). If gas is heated near the black hole, less accretion is expected. It is likely that cosmic rays and magnetic fields are relevant, since the cores of almost all massive elliptical galaxies are sites of low-luminosity nonthermal radio emission (e.g., Sadler et al. 1994). Powerful radio jets are typically found in rich clusters, not in (the more numerous) small groups that contain central elliptical galaxies of comparable optical luminosity. Jets that deposit energy asymmetrically and to very large radii are an unlikely heating source for groups such as NGC 5044 and RGH 80. By contrast, the heating required in our circulation flows is isotropic and requires a modest, approximately continuous AGN power.

In our discussion of steady state circulation flows (Mathews et al. 2003), we describe limits on the size and mass of bubbles if heating occurs at some radius r_h in the flow. Provided they remain coherent, larger bubbles can move to larger radii, but the size of new bubbles cannot exceed the radius r_h where they are formed, and this in turn limits the global rate at which mass can be buoyantly transported outward. We discussed these difficulties in the context of steady state circulation, and they did not critically impair the circulation model. In this first paper on time-dependent circulation, we have not discussed again all these important considerations. The insensitivity of circulation flows to the filling factor also lessens the urgency for a fully self-consistent model for the rising bubbles, even if that were possible. Nevertheless, as we computed these circulation flows, our concept of the heating radius r_h became more flexible. We consider r_h to be only a representative radius at which the gas is heated. Larger and smaller clouds can be heated and formed at larger and smaller radii, respectively. In reality, the heating probably occurs throughout a volume that may vary with time.

A critical measure of the success of circulation flows is the apparent rise in the gas temperature toward a maximum well outside the central elliptical galaxy. This $T(r)$ is possible only if the emission from the high-density cooling inflow dominates the observed temperature profile in the inner flow, even when the mass flux carried by the rising bubbles transports nearly the same mass outward. We showed that this is indeed the case for steady state circulation flows (Mathews et al. 2003). To see why this is also true for time-dependent circulations, we estimate the ratio of the bubble to cooling flow bolometric X-ray emissivities at $r = r_h$ at time $t = t_n$,

$$\frac{\epsilon_{b,h}}{\epsilon_h} = \left(\frac{\rho_{b,h}}{\rho_h}\right)^2 \frac{\Lambda(T_{b,h})}{\Lambda(T_h)} \frac{1 - f(r_h)}{f(r_h)}. \tag{29}$$

The bubble density at r_h can be estimated from the steady state equation for mass conservation,

$$\rho_{b,h} \approx \frac{\left(|\dot{M}_h| + \dot{M}_*\right)}{4\pi r_h^2 [1 - f(r_h)]} \frac{1}{u_{b,h}}, \tag{30}$$

where $u_{b,h}$ is the typical velocity of rising bubbles near r_h. Using the flow parameters for the $(m,\ n,\ r_{p,\rm kpc},\ \epsilon_h) = (1,\ 1.5,\ 30,\ 2.0)$ flow at time t_n, we find $\rho_{b,h} = 2.3 \times 10^{-26}/u_{b,h2}$ g cm^{-3}, where $u_{b,h2}$ is the bubble velocity in units of 100 km s^{-1}. The bubble temperature $T_{b,h} = 1.5 \times 10^7 u_{b,h2}$ K follows from pressure equilibrium. With these values we find $\epsilon_{b,h}/\epsilon_h \approx 0.06/u_{b,h2}^2 \approx 0.007 \ll 1$ if $u_{b,h2} = 3$, a typical initial bubble velocity in the steady flows of Mathews et al. (2003). Therefore, emission from the cooling inflow dominates the observed $T(r)$ and the bolometric X-ray emission near the center of this flow. X-ray spectral features from heated gas may be emitted mostly by somewhat denser gas at intermediate temperatures, $T_h < T < T_{b,h}$.

There are two stages of heating in our circulation flows. Near the center $r \sim r_h$, we assume a strong and concentrated heating by an AGN that rather sharply raises the entropy, creating buoyant bubbles of hot gas. This is regarded as the primary heating mechanism. A second heating process occurs when the rising bubbles share some of this thermal energy with the inflowing gas over a large region of the flow. Without this distributed heating, the entropy profile in the gas fails to match the observations (as in Fig. 4). Distributed heating

occurs because of bubble-flow drag or because some of the outflowing gas thermally merges with the incoming flow before it reaches the radius where the initial entropy of the bubble equals that of the ambient flow. This distributed heating helps determine the location of the temperature maximum observed in the flow. Finally, it is not surprising that the central heating exceeds L_h by some factor $\epsilon_h \sim 2.0$ because (1) the mean heating factor $\langle h \rangle$ is underestimated if some of the bubble energy is prematurely transferred to the inflowing gas, (2) some of the bubble energy is lost by radiation and this is necessary to explain the superiority of two-temperature fits to the X-ray spectra, and (3) the kinetic energy acquired by the bubbles is extracted from the galaxy-group potential and is independent of L_h.

X-ray observations of the Perseus cluster show buoyant cavities that have moved through distances that are 10–15 times larger than the cavity diameters (e.g., Fabian et al. 2000). The coherence of these large bubbles is remarkable, and they appear to be transporting mass and heated gas to large radii in the flow. Since small buoyant regions experience more drag as they move upstream through the cooling flow, their rate of progress may not be sufficient to convey the mass and energy that we require in the models described here. Clearly, observational and computational studies of the physical coherence of heated regions will be necessary to fully validate circulation flows. The dynamical coherence of heated bubbles may result from internal magnetic fields that are force free.

It is possible that some gas cools. For NGC 5044, $r_h = 5$ kpc, taken literally, is about $R_e/2$, so we expect $\sim 0.1\ M_\odot\ \mathrm{yr}^{-1}$ from stellar mass loss within r_h. Even if this gas cools radiatively in the usual manner, such a small cooling rate would not have been detected in our *XMM* observations (Buote et al. 2003a). However, cooling in this core region is likely to be accelerated by electron–dust grain cooling during which X-rays are emitted at a much reduced level (Mathews & Brighenti 2003a). Central (dust-enhanced) cooling may consume $\sim 10\%$ of the iron produced by SNeIa.

6. CONCLUSIONS

In this paper we describe a new model for the dynamical evolution of hot gas in groups and clusters of galaxies in which gas flows in both radial directions simultaneously. The incoming gas resembles a traditional cooling flow and dominates the X-ray emission. The outgoing gas consists of an ensemble of heated buoyant bubbles that rise to distant regions where they merge with the inflowing gas. We have not calculated the dynamics of the rising bubbles of heated gas in detail, and this must be an objective for the future. Instead, we constructed a schematic time-dependent model guided in part by observations and by the detailed bubble-flow interactions described in our previous study of steady state circulation flows (Mathews et al. 2003). It is noteworthy and fortunate that the density and temperature profiles of the cooling, inflowing gas are not sensitive to the filling factor $f(r)$, which is easier to determine reliably from the observations than from dynamical models for the bubbles. This insensitivity may explain the approximate similarity of $T(r)$ and $n_e(r)$ profiles in clusters of all sizes.

We have shown here that the steady state circulation flows we proposed earlier (Mathews et al. 2003) can be generalized to include time variation. An essential feature of successful circulation flows is that both mass and energy must be distributed from the center throughout a large volume of the flow within the cooling radius. The outward increase in gas temperature near the center of the flow, a characteristic feature of most galaxy clusters, results largely from a conventional cooling inflow, modified somewhat by additional energy received from locally outflowing bubbles. After evolving for many gigayears, circulation flows are in accord with the important observation that most or all of the iron produced by SNeIa in the central elliptical galaxy has been stored in a region typically extending to ~ 100 kpc. From the perspective of the circulation flow hypothesis, a record of the enrichment-heating history of groups is retained in the currently observed iron and temperature profiles of the hot gas, and it may be possible to retrieve this information by comparison with more accurate circulation flows.

The central peak in the radial iron distribution within ~ 50 kpc is very sensitive to the (negative) cooling inflow velocity at small radii. If this velocity is high, the iron abundance remains low and flat-topped. Iron abundance profiles that peak sharply toward the center, such as that observed in NGC 5044, can occur only if the flow velocity is reduced to a very low level by (recent) large heating near the center. We have shown that the central iron peak is more pronounced when the mass redistribution and heating are more strongly peaked at smaller radii.

Concentrated peaks in the iron abundance within ~ 100 kpc are also typically observed in many rich clusters: Sersic 159-03 (Kaastra et al. 2001), Cygnus A (Smith et al. 2002), A1795 (Ettori et al. 2002), and A2029 (Lewis et al. 2002). We speculate that these regions are also mostly enriched by the circulation of iron from SNeIa in the central galaxies, and there is some observational support for this (e.g., Ettori et al. 2002). If so, this may indicate a characteristic heating luminosity $L_h \sim 10^{42}-10^{43}$ ergs s^{-1} for all clusters. However, if there is an upper limit on the heating luminosity L_h, perhaps set by the physical conditions near the central black hole, it is possible that the mass inflow rate $|\dot{M}|$ in rich clusters will be too large for the inflowing gas to be heated in the way we describe here. This may give rise to additional, more violent energy releases in the form of powerful radio jets, which are rare in galaxy groups that have more modest mass cooling rates $|\dot{M}|$.

We believe the circulation flows described here are the first gasdynamic, long-term evolutionary models that are in good agreement with all essential features of the hot gas: the gas temperature maximum at several R_e, the approximately linear rise of entropy with radius, the dominance of SNIa products in the X-ray spectra, the total iron mass within 100 kpc, and its radial distribution. The relative constancy of these observed profiles during the many gigayears of our calculated flows is consistent with the similarity of the observed X-ray properties among galaxy groups and clusters. Finally, little or no gas cools in circulation models, and this is consistent with the much decreased or absent cooling gas in X-ray spectra of both galaxy groups and clusters.

These studies of the evolution of hot gas in elliptical galaxies at the University of California, Santa Cruz, are supported by NASA grants NAG5-8409 and ATP 02-0122-0079 and NSF grants AST 98-02994 and AST 00-98351, for which we are very grateful.

REFERENCES

Blanton, E. L., Sarazin, C. L., & McNamara, B. R. 2003, ApJ, 585, 227
Brighenti, F., & Mathews, W. G. 2002, ApJ, 573, 542
———. 2003, ApJ, 587, 580
Buote, D. A. 2000a, ApJ, 539, 172
———. 2000b, MNRAS, 311, 176
Buote, D. A., Brighenti, F., & Mathews, W. G. 2004, ApJ, 607, L91
Buote, D. A., Lewis, A. D., Brighenti, F., & Mathews, W. G. 2003a, ApJ, 594, 741
———. 2003b, ApJ, 595, 151
Cappellaro, E., Evans, R., & Turatto, M. 1999, A&A, 351, 459
De Grandi, S., Ettori, S., Monghetti, M., & Molendi, S. 2004, A&A, 419, 7
De Grandi, S., & Molendi, S. 2001, ApJ, 551, 153
Dupke, R. A., & White, R. E., III. 2003, ApJ, 583, L13
Ettori, S., Fabian, A. C., Allen, S. W., & Johnstone, R. M. 2002, MNRAS, 331, 635
Fabian, A. C., et al. 2000, MNRAS, 318, L65
Gal-Yam, A., & Maoz, D. 2004, MNRAS, 347, 942
Gastaldello, F., & Molendi, S. 2002, ApJ, 572, 160
Johnstone, R. M., Allen, S. W., Fabian, A. C., & Sanders, J. S. 2002, MNRAS, 336, 299
Kaastra, J. S., Ferrigno, C., Tamura, T., Paerels, F. B. S., Peterson, J. R., & Mittaz, J. P. D. 2001, A&A, 365, L99
Kim, D.-W., & Fabbiano, G. 2004, ApJ, 613, 933
Lewis, A. D., Stocke, J. T., & Buote, D. A. 2002, ApJ, 573, L13
Loewenstein, M., Mushotzky, R. F., Angelini, L., Arnaud, K. A., & Quataert, E. 2001, ApJ, 555, L21
Loken, C., Norman, M. L., Nelson, E., Bryan, G. L., & Motl, P. 2002, ApJ, 579, 571
Mathews, W. G. 1989, AJ, 97, 42
———. 1997, AJ, 113, 755
Mathews, W. G., & Brighenti, F. 2003a, ApJ 590, 5
———. 2003b, ARA&A, 41, 191
Mathews, W. G., Brighenti, F., Buote, D. A., & Lewis, A. D. 2003, ApJ, 596, 159
Morris, R. G., & Fabian, A. C. 2003, MNRAS, 338, 824
Navarro, J., Frenk, C., & White, S. 1997, ApJ, 490, 493
O'Sullivan, E., Vrtilek, J. M., Read, A. M., David, L. P., & Ponman, T. J. 2003, MNRAS, 346, 525
Pain, R., et al. 2002, ApJ, 577, 120
Peterson, J. R., et al. 2001, A&A, 365, L104
Rickes, M. G., Pastoriza, M. G., & Bonatto, C. 2004, A&A, 419, 449
Sadler, E. M., Slee, O. B., Reynolds, J. E., & Ekers, R. D. 1994, in ASP Conf. Ser. 54, The First Stromlo Symposium: The Physics of Active Galaxies, ed. G. V. Bicknell, M. A. Dopita, & P. J. Quinn (San Francisco: ASP), 335
Sanders, J. S., & Fabian, A. C. 2002, MNRAS, 331, 273
Schmidt, R. W., Fabian A. C., & Sanders, J. S. 2002, MNRAS, 337, 71
Smith, D. A., Wilson, A. S., Arnaud, K. A., Terashima, Y., & Young, A. J. 2002, ApJ, 565, 195
Stone, J. M., & Norman, M. L. 1992, ApJS, 80, 753
Sun, M., Forman, W., Vikhlinin, A., Hornstrup, A., Jones, C., & Murray, S. S. 2003, ApJ, 598, 250
Sutherland, R. S., & Dopita, M. A. 1993, ApJS, 88, 253
Xu, H., et al. 2002, ApJ, 579, 600
Xue, Y.-J., Böhringer, H., & Matsushita, K. 2004, A&A, 420, 833